Bioorganic & Medicinal Chemistry 19 (2011) 5935–5947

Contents lists available at SciVerse ScienceDirect

Bioorganic & Medicinal Chemistry

journal homepage: www.elsevier.com/locate/bmc

Structure-based design of dipeptide derivatives for the human neutral endopeptidase

Kensuke Misawa [a,*], Yasuto Suzuki [a], Satoshi Takahashi [b], Atsushi Yoshimori [b], Ryoko Takasawa [c], Yusuke Shibuya [a], Sei-ichi Tanuma [c,d]

[a] Biological Science Laboratories, Kao Corporation, 2606 Akabane, Ichikai-machi, Haga-gun, Tochigi 321-3497, Japan
[b] Institute for Theoretical Medicine Inc., Tokyo Institute of Technology, Yokohama Venture Plaza W101, 4259-3 Nagatsuda, Midori-ku, Yokohama, Kanagawa 226-8510, Japan
[c] Department of Biochemistry, Faculty of Pharmaceutical Sciences, Tokyo University of Science, 2641 Yamazaki, Noda, Chiba 278-8510, Japan
[d] Genome and Drug Research Center, Tokyo University of Science, 2641 Yamazaki, Noda, Chiba 278-8510, Japan

ARTICLE INFO

Article history:
Received 30 June 2011
Revised 26 August 2011
Accepted 27 August 2011
Available online 1 September 2011

Keywords:
Neutral endopeptidase
Inhibitor
Structure-based drug design
Structure–activity relationship
In silico

ABSTRACT

Neutral endopeptidase (NEP) plays a key role in the metabolic inactivation of various bioactive peptides such as atrial natriuretic peptide (ANP), endothelins, and enkephalins. Furthermore, NEP is known to work as elastase in skin fibroblast. Therefore, effective inhibitors of NEP offer significant therapeutic interest as antihypertensives, analgesics, and skin anti-aging agents. Recently, the X-ray crystal structure of human NEP complexed with phosphoramidon has been reported and provided insights into the active site specificity of NEP. Here, we designed new inhibitors by using in silico molecular modeling and synthesized them by short steps. Expectedly, we found highly effective inhibitors with sub-nanomolar levels of IC_{50} values. These results indicate that our structure-based molecular designing program is useful for obtaining novel NEP inhibitors. Furthermore, these inhibitors may be attractive leads for the generation of new pharmaceuticals for NEP-related diseases.

1. Introduction

Neutral endopeptidase (NEP; EC 3.4.24.11), known as neprilysin or enkephalinase, is a mammalian type II integral membrane zinc-containing endopeptidase (M13 family) and widely distributed in various mammalian tissues such as brain, heart, kidney, lung, and skin.[1–5] NEP plays an important role in the regulation of opioid peptides action through the degradation of enkephalins and substance P in the nervous system.[3] NEP is also involved in the degradation of the cardiovascular peptides such as atrial natriuretic peptide (ANP), endothelins, and bradykinin in the cardiovascular system.[4] Furthermore, NEP is known to work as elastase in skin fibroblast.[5] Therefore, NEP is a therapeutic potential target as analgesics, antihypertensives, and skin anti-aging agents.[5–7]

So far, NEP inhibitors have been developed together with angiotensin-converting enzyme (ACE) or endothelin-converting enzyme-1 (ECE-1) inhibitors.[6,8] For example, racecadotril, which is rapidly metabolized to its active metabolite thiorphan, is a NEP inhibitor used in clinical practice for diarrhea.[9] Moreover, omapatrilat is a mixed NEP/ACE dual inhibitor developed for beneficial effects in the management of hypertension.[8] However, since there are still side-effects derived from the low specificities and non-specific metal-chelating groups like thiorphan, the generation of new highly effective NEP inhibitors is needed for the development of NEP-related diseases such as analgesics, antihypertensives, and skin anti-aging agents.

Recently, the X-ray crystal structure of human NEP complexed with phosphoramidon has been reported and provided insights into the structure of the active site of NEP.[10] Previously, we developed a peptide derivative, *N*-(carboxymethyl)-L-phenylalanyl-β-alanine (compound **1**), as a NEP inhibitor (Fig. 1).[11] Thus, we attempted to design computationally more effective inhibitors based on the scaffold of compound **1**. In this study, we synthesized in silico designed derivatives from compound **1** and examined their inhibitory effects on human NEP. Importantly, we could design new-type more effective inhibitors that have sub-nanomolar levels of IC_{50} values. These results indicate the usefulness of our molecular modeling program for designing NEP inhibitors. Furthermore, these inhibitors may open a new way to develop novel pharmaceuticals for NEP-related diseases such as analgesics, antihypertensives, and skin anti-aging agents.

2. Results

2.1. Predicting the binding mode of compound 1 with NEP

In order to design new derivatives of compound **1**, we analyzed the molecular recognition of NEP-ligand. We used the molecular

* Corresponding author. Tel.: +81 285 68 7573; fax: +81 285 68 7523.
E-mail address: misawa.kensuke@kao.co.jp (K. Misawa).

0968-0896/$ - see front matter © 2011 Elsevier Ltd. All rights reserved.
doi:10.1016/j.bmc.2011.08.064

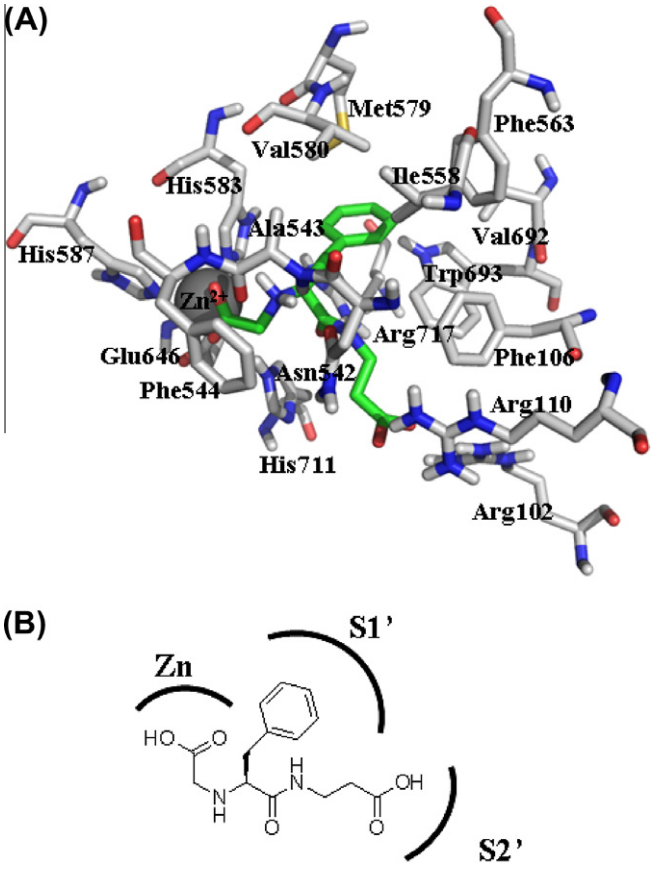

Figure 1. The predicted binding mode of compound **1** to the active site of human NEP. The binding mode was obtained from docking simulation. Nitrogen, oxygen, and carbon atoms of inhibitors are blue, red, and green, respectively (A). The predicted interaction of compound **1** to the active site of NEP in a schematic view (B).

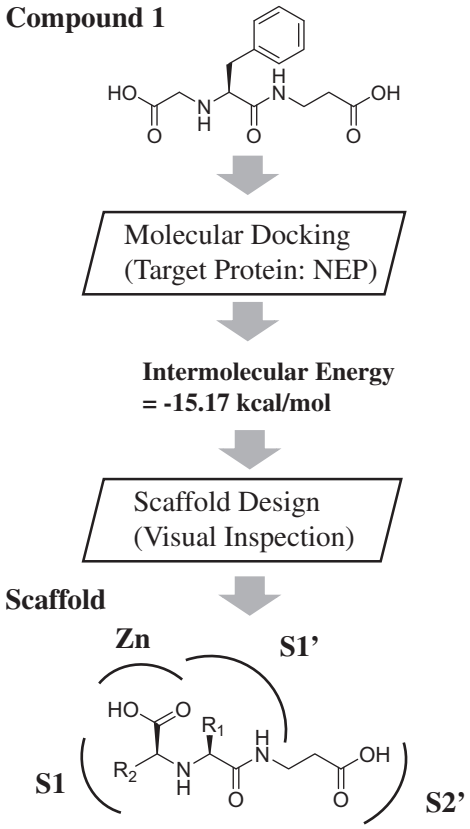

Figure 2. The chemical structure of compound **1** and the designing scaffold.

modeling package AutoDock 4.2[12] and the X-ray crystal structure of human NEP complexed with MCB3937 (PDB: 2QPJ).[13]

Figure 1 shows that the N-terminal carboxyl group of compound **1** binds to the catalytically active zinc(II) ion, ligated to the side chains of His583, His587, and Glu646. The phenyl group was expected to fill the hydrophobic pocket S1′ (Fig. 1B), defined by Ile558, Phe563, Met579, Val580, Val692, and Trp693 (Fig. 1A). The C-terminal carboxyl group was hoped to interact with S2′ pocket (Fig. 1B), defined by Arg102, Phe106, Arg110, and Asn542, by forming hydrogen bonds with Arg102 and Arg110 (Fig. 1A). To obtain more potent inhibitors, we tried to design a new scaffold that fills the hydrophobic pockets S1 defined by Phe544 and S1′ more effectively (Fig. 2).

2.2. Computational designing of NEP inhibitors

In order to optimize the functional groups (R_1 and R_2) step-wisely, we first constructed scaffold A and used our in-house library composed of the 68 commercially available amino acid derivatives (Fig. 3). The molecular docking was performed by using the NEP structure (PDB: 2QPJ). As a result, compound **2**, which has the biphenylmethyl group (Frag ID: **AD23**), had the lowest intermolecular energy (Table 1).

Next, we constructed scaffold B to optimize R_2 and used our in-house small and hydrophobic fragments library composed of the 8 possible amino acids, since R_2 was expected to interact with Phe544 located in the S1 subsite (Table 2). As shown in Figure 4, compound **3**, which has the phenylethyl group (Frag ID: **SH07**), could deeply interact with S1 pocket. Among the designed compounds, compound **3** had the lowest intermolecular energy. Thus, we decided to synthesize compound **3** as a new candidate of NEP inhibitor. Also, we prepared compounds **2** and **4**–**6** to evaluate their structure–activity relationship (SAR).

2.3. Chemical synthesis of designed compounds

The synthetic route of compound **2** is illustrated in Scheme 1. Coupling of compound **7** with the *N*-Boc amino acid gave compound **8**. The deprotection of the Boc group of compound **8** with HCl/1,4-dioxane provided compound **9**. Compound **9** was treated with benzyl bromoacetate to give compound **10**. Hydrogenolysis of the two benzyl ester groups of compound **10** gave compound **2**.

Scheme 2 shows the synthetic routes of compounds **3**–**5**. The protection of *N*-Boc β-amino acid derivative **11** with benzyl ester and the deprotection of the Boc group with HCl/1,4-dioxane provided compound **13**. Coupling of compound **7** or **13** with the *N*-Boc amino acid and the deprotection of the Boc group with formic acid provided compounds **16a**–**c**. Compounds **16a**–**c** were treated with the triflate, prepared from commercially available (*R*)-2-hydroxy-4-phenylbutyric acid,[14] to give compounds **17a**–**c**. Hydrogenolysis of the two benzyl ester groups of compounds **17a**–**c** gave compounds **3**–**5**.

Scheme 3 shows the synthetic route of compound **6**. The protection of *N*-Boc β-amino acid derivative **18** with benzyl ester and the deprotection of the Boc group with formic acid provided compound **20**. Compound **20** was treated with the triflate, prepared

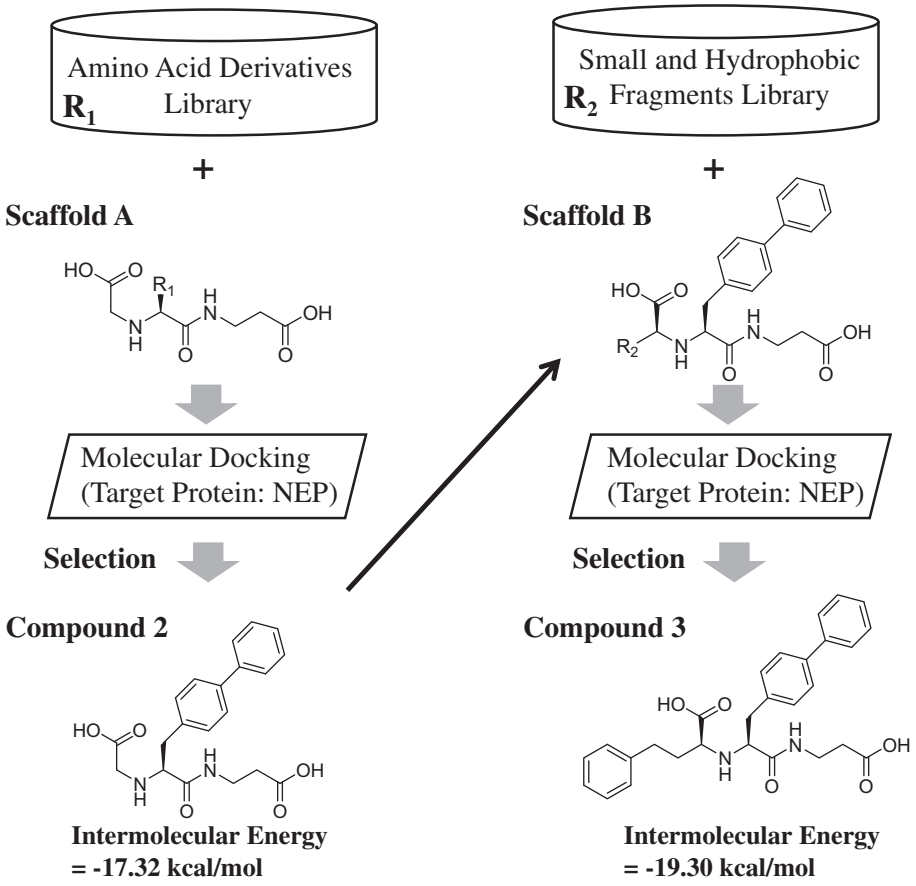

Figure 3. The scheme of designing and optimizing new NEP inhibitors by using scaffolds A and B.

from commercially available (*R*)-2-hydroxy-4-phenylbutyric acid,[14] to give compound **21**. Hydrogenolysis of the two benzyl ester groups of compound **21** gave compound **6**.

2.4. Effects of compound 1 derivatives on human NEP activity

The NEP interaction energies and its inhibitory effects of compound **1** derivatives are summarized in Table 3. The IC_{50} values were determined by a fluorometric assay.[15] The correlation coefficient of R^2 between the intermolecular energies and the IC_{50} values was calculated to be 0.83 (Fig. 5). Interestingly, compound **3** was proved to be a very potential inhibitor with the IC_{50} value of 0.36 nM. Compound **4**, which has the methyl moiety at α-position of β-alanine, had roughly the same inhibitory effect as compound **3**. This suggests that the methyl group, which is expected to have the hydrophobic interaction with Phe106 in the S2′ pocket (Fig. 4), contributes little to its inhibitory potency. In contrast, compound **2**, which is lack of the phenylethyl group of compound **3**, had approximate 30-fold weaker inhibitory activity than compound **3**. This implies that the phenylethyl moiety of compound **3** has the hydrophobic interaction with Phe544 in the S1 subsite.

Compound **5**, which does not have the second phenyl group of compound **4**, showed about 800-fold weaker inhibitory activity than compound **4**. This indicates that the S1′ pocket, which is formed by the side chains of Ile558, Phe563, Met579, Val580, Val692, and Trp693, is deep and hydrophobic, and could accommodate a large group like biphenyl.[16] On the other hand, compound **6**, which lacks β-alanine moiety, had about 1200-fold weaker inhibitory activity than compound **3**. This suggests that the C-terminal carboxyl group interacts with the polar amino acids such as Arg102 and Arg110 in the S2′ subsite.

3. Discussion

In this study, we attempted to design unique NEP inhibitors by using the scaffold based on the binding mode of compound **1** and analyzed their structure–activity relationship (SAR). The biphenylalanyl-β-alanine structure is already used for NEP inhibitor such as the compounds developed by Schering–Plough[17] and Ciba–Geigy.[18] However, the phenylethyl group modification with the biphenylalanyl-β-alanine structure in compounds **3** and **4** is a new one, and contributes to their highly inhibitory potencies. Indeed, compounds **3** and **4** have sub-nanomolar levels of IC_{50} values of 0.36 and 0.51 nM, respectively. This suggests that the compounds modified with the phenylethyl group are more effective than those having only the biphenylalanyl-β-alanine structure like compound **2**.

Table 3 shows the calculated molecular interaction energies and the IC_{50} values of compounds **1**–**6**. Also, Figure 5 shows that the correlation coefficient of R^2 between the intermolecular energies and the IC_{50} values is 0.83. The results suggest a good correlation between the calculated interaction energies and the inhibitory activities. Thus, these observations indicate the validity of this molecular design program for the development of effective NEP inhibitors. Furthermore, we performed the decomposition analysis based on MM-GB/SA method in order to define the hot spot amino acid residues of human NEP. The contribution of each amino acid to the interaction with the compounds was evaluated and the 9 amino acids (Arg102, Arg110, Asn542, Ala543, Phe544, Val580, Val692,

Table 1
The calculated intermolecular energies of compounds **AD01–68** based on scaffold A

Frag ID	R_1	Intermolecular energy (kcal/mol)	Frag ID	R_1	Intermolecular energy (kcal/mol)
AD01		−12.36	**AD35**	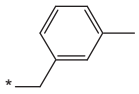	−14.91
AD02		−12.37	**AD36**	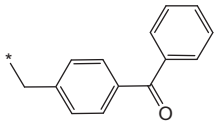	−13.55
AD03		−11.64	**AD37**	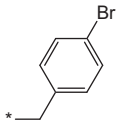	−15.24
AD04		−12.48	**AD38**	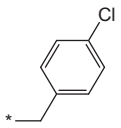	−14.53
AD05		−13.81	**AD39**	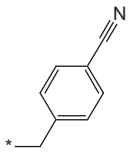	−14.93
AD06	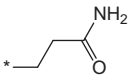	−12.17	**AD40**	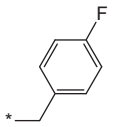	−13.85
AD07	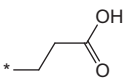	−13.08	**AD41**	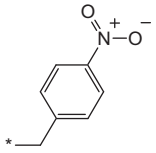	−14.35
AD08		−12.08	**AD42**	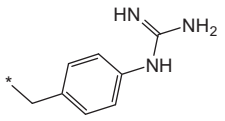	−16.07
AD09	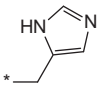	−13.83	**AD43**	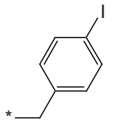	−15.34
AD10		−14.47	**AD44**	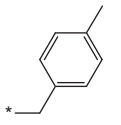	−15.22
AD11		−13.19	**AD45**	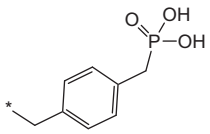	−13.22
AD12	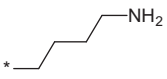	−13.76	**AD46**	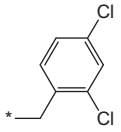	−14.94
AD13	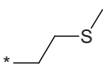	−13.14	**AD47**	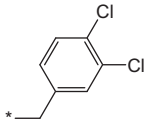	−14.16

Table 1 (*continued*)

Frag ID	R_1	Intermolecular energy (kcal/mol)	Frag ID	R_1	Intermolecular energy (kcal/mol)
AD14		−12.84	**AD48**	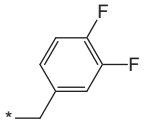	−14.58
AD15		−11.54	**AD49**	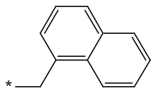	−14.11
AD16		−12.41	**AD50**	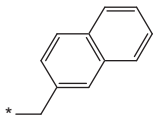	−13.72
AD17	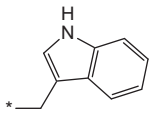	−15.06	**AD51**	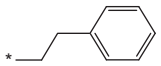	−14.69
AD18	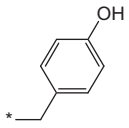	−15.08	**AD52**	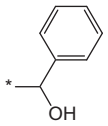	−13.51
AD19		−13.23	**AD53**	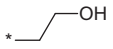	−13.03
AD20	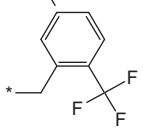	−15.21	**AD54**	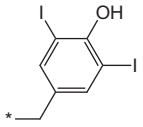	−13.21
AD21	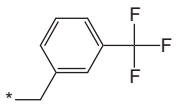	−12.80	**AD55**	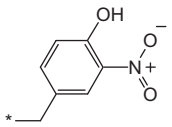	−14.22
AD22	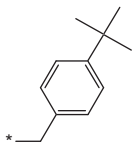	−13.62	**AD56**	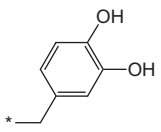	−13.75
AD23[**]	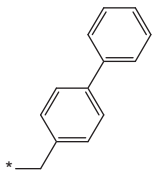	−17.32	**AD57**	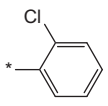	−13.61
AD24	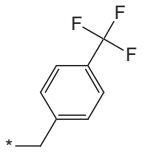	−14.30	**AD58**	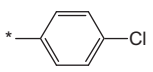	−13.65
AD25	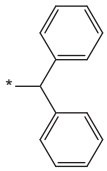	−10.30	**AD59**	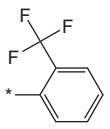	−11.93
AD26	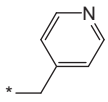	−14.62	**AD60**	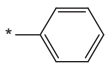	−13.39

(*continued on next page*)

Table 1 (*continued*)

Frag ID	R_1	Intermolecular energy (kcal/mol)	Frag ID	R_1	Intermolecular energy (kcal/mol)
AD27	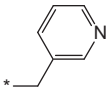	−13.71	**AD61**	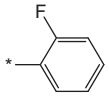	−13.36
AD28	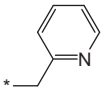	−14.66	**AD62**	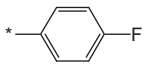	−12.98
AD29	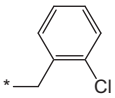	−16.01	**AD63**	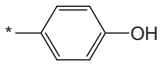	−13.14
AD30	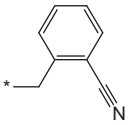	−15.38	**AD64**		−13.92
AD31	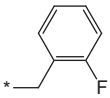	−14.12	**AD65**	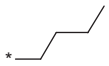	−13.42
AD32	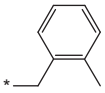	−15.50	**AD66**		−12.58
AD33	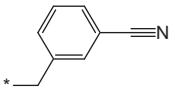	−13.75	**AD67**	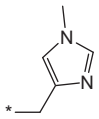	−13.11
AD34	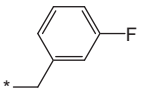	−14.11	**AD68**	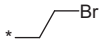	−13.14

** Compound **2**.

Table 2
The calculated intermolecular energies of compounds **SH01–08** based on scaffold B

Frag ID	R_2	Intermolecular energy (kcal/mol)
SH01		−17.34
SH02		−15.59
SH03	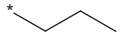	−17.88
SH04	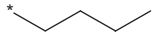	−15.30
SH05	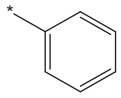	−17.01
SH06	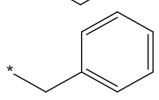	−17.67
SH07**	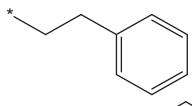	−19.30
SH08	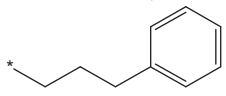	−12.78

** Compound **3**.

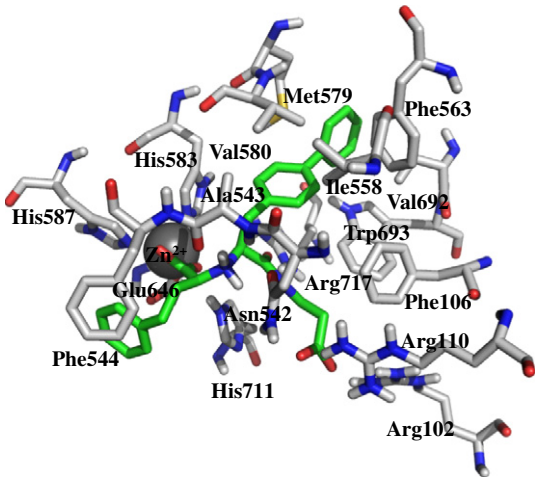

Figure 4. The predicted binding mode of compound **3** to the active site of human NEP. The binding mode was obtained from docking simulation. Nitrogen, oxygen, and carbon atoms of inhibitors are blue, red, and green, respectively.

His711, and Arg717) were determined as hot spot amino acid residues (except for His583, His587, and Glu646, which are consisted of the catalytic site). Figure 6 shows the comparison of the binding free energy of each amino acid when compound **1** or **3** binds to human NEP. This suggests the preferential interaction between compound **3** and human NEP.

There are a few reasons for the higher inhibitory potency of compound **3**. First, the C-terminal carboxyl group interacts with Arg102 and Arg110, and the amide of compound **3** interacts with Asn542 and Arg717 by forming hydrogen bonds, resulting that

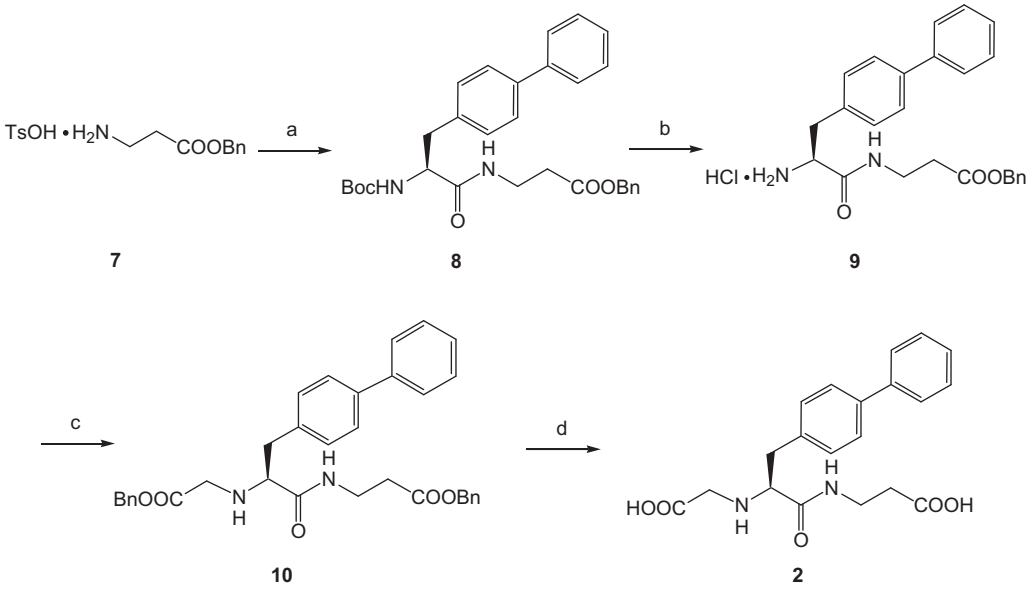

Scheme 1. The synthesis of compound **2**. Reagents and conditions: (a) *N*-Boc amino acid, WSC·HCl, HOBt, NMM, DMF, 0 °C to rt; (b) 4 N HCl/1,4-dioxane; (c) benzyl bromoacetate, Et_3N, THF; (d) H_2, Pd/C, MeOH.

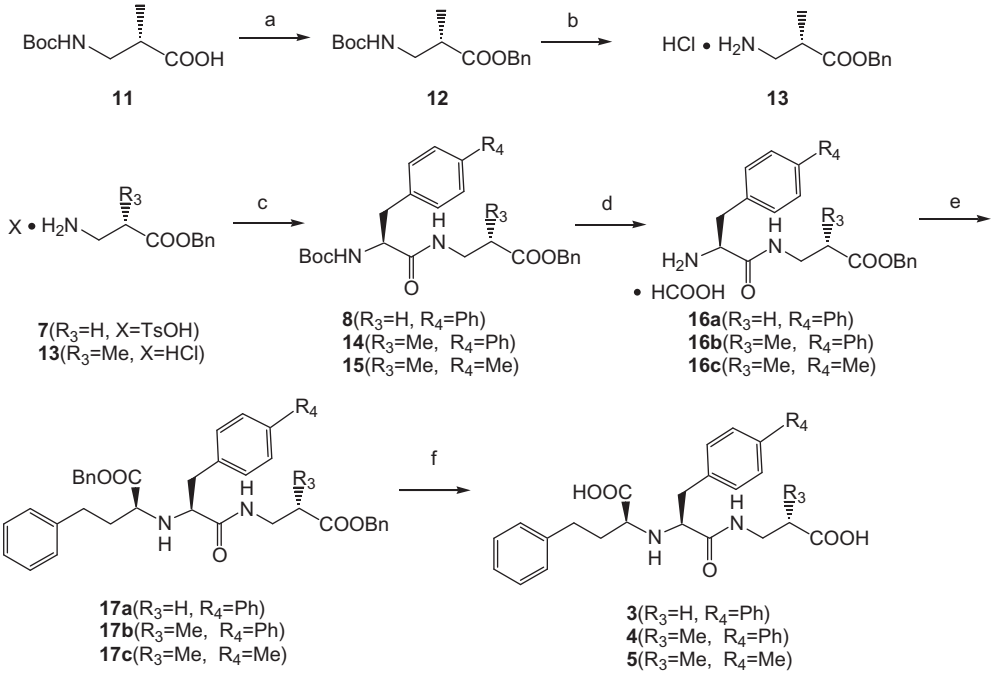

Scheme 2. The synthesis of compounds **3**–**5**. Reagents and conditions: (a) BnOH, DMAP, WSC·HCl, $CHCl_3$, 0 °C to rt; (b) 4 N HCl/1,4-dioxane; (c) *N*-Boc amino acid, WSC·HCl, HOBt, NMM, DMF, 0 °C to rt; (d) HCOOH; (e) (*R*)-2-hydroxy-4-phenylbutyric acid benzyl ester, Tf_2O, Et_3N, CH_2Cl_2, −78 °C; then **16a**–**c**, −78 °C to rt; (f) H_2, Pd/C, DMF or AcOH/MeOH/H_2O (6/3/1).

they contribute largely to the total reduction of the binding free energy. Compound **6**, which is lack of β-alanine moiety, has about 1200-fold weaker inhibitory activity than compound **3**, suggesting that the interaction with Arg102 and Arg110 contributes to the higher inhibitory potency. Second, the phenylethyl moiety interacts with Phe544 in the S1 subsite. Compound **2**, which lacks the phenylethyl group of compound **3**, had approximately 30-fold weaker inhibitory activity than compound **3**, implying that the hydrophobic interaction with Phe544 is involved in the higher inhibitory potency. Third, the second phenyl ring of the biphenyl group interacts tightly with Val692 in the S1′ subsite. Compound **5**, which does not have the second phenyl group of compound **4**, showed about 800-fold weaker inhibitory activity than compound **4**, suggesting that the hydrophobic interaction with Val692 contributes to the higher inhibitory potency. Fourth, the secondary amine moiety of compound **3** interacts with the carbonyl group of Ala543 by forming hydrogen bond, resulting from the conformational changes arising from the biphenyl group and thereby the interaction with Phe544. The binding free energy of Ala543 reduced more efficiently when compound **3** bound to NEP, as

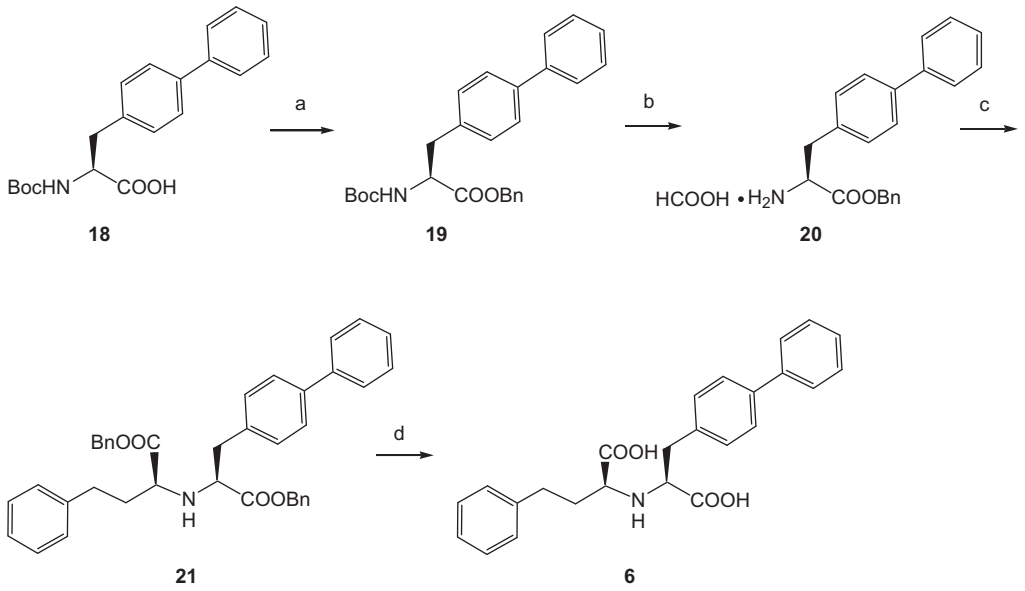

Scheme 3. The synthesis of compound **6**. Reagents and conditions: (a) BnOH, DMAP, WSC·HCl, $CHCl_3$, 0 °C to rt; (b) HCOOH; (c) (*R*)-2-hydroxy-4-phenylbutyric acid benzyl ester, Tf_2O, Et_3N, CH_2Cl_2, −78 °C; then **20**, −78 °C to rt; (d) H_2, Pd/C, DMF.

compared with that of compound **1**, implying the tight interaction of the secondary amine moiety of compound **3** with the carbonyl group of Ala543.

4. Conclusion

In this report, we showed the novel pharmacophore model for NEP inhibitors. Based on this model, a new series of NEP inhibitors was designed, synthesized, and evaluated for their inhibitory activities. Consequently, compound **3** was identified as the highest effective inhibitor with the IC_{50} value of 0.36 nM. Furthermore, we analyzed the SAR by performing the decomposition analysis based on MM-GB/SA method. Importantly, the 9 amino acids could be identified as hot spot amino acid residues that are involved in the inhibitory potencies. Thus, our model may be useful for screening and designing of effective NEP inhibitors for the creation of new pharmaceuticals.

5. Materials and methods

Melting points (mp) were determined on a Büchi B-535 apparatus and were uncorrected. IR spectra were recorded on a PerkinElmer Spectrum One (ATR). ^{1}H NMR were recorded on a Bruker AVANCE III 600 MHz spectrometer and ^{13}C NMR spectra were recorded on a Bruker AVANCE III 150 MHz. ^{1}H chemical shifts are expressed in parts per million (ppm) based on internal TMS (0.00 ppm). ^{13}C chemical shifts are expressed in parts per million (ppm) based on internal TMS (0.00 ppm). High resolution mass spectra (HRMS) were recorded on a ThermoFisher LTQ Orbitrap Discovery with electron spray ionization (ESI). All reagents and solvents were of commercial quality from freshly opened containers and were used without further purification. Reaction progress was monitored by analytical thin layer chromatography (TLC) on pre-coated glass plates (silica gel 60 F_{254} Merck) and products were visualized by UV light and phosphomolybdic acid hydrate in EtOH with heating. Column chromatography was accomplished on Hiflash column (silica gel, Yamazen Science Inc.). The reaction temperatures are indicated as the temperature of the oil bath. Purity of compounds was determined by means of UFLC with a Shimadzu liquid chromatographic system consisting of a CBM-20A system controller, LC-20AD pump, SPD-M20A UV spectrophotometric detector, SIL-20AC autoinjector, CTO-20AC column oven, and DGU-20A3 degasser. The samples (each 4 μL) were injected using a refrigerated autosampler kept at 20 °C. The chromatographic analyses were carried out on a Shim-Pack XR-ODS (3.0 i.d. × 50 mm, 2.2 μm, Shimadzu) kept at 40 °C, using acetonitrile: 0.1(v/v)% TFA/H_2O (t = 0 min, 20:80; t = 0.7 min, 20:80; t = 5.7 min, 100:0; t = 6.4 min, 100:0) as a mobile phase. The flow rate was 1 mL/min and the absorbance at 220 nm was monitored.

5.1. Synthesis

5.1.1. *N*-(Carboxymethyl)-L-phenylalanyl-β-alanine (1)

Compound **1** was synthesized according to the previous methods.[11]

White crystals. UFLC: >99% purity. mp: 166.4–168.8 °C (dec.) (recrystallization from 20% IPA aq). IR (ATR, cm^{-1}) ν 3285, 3030, 1667, 1622, 1555, 1392, 1199, 746, 699. ^{1}H NMR (DMSO-d_6, δ ppm): 2.30 (2H, m), 2.76 (1H, dd, J = 7.4, 13.6 Hz), 2.87 (1H, dd, J = 6.2, 13.6 Hz), 3.06 (1H, d, J = 17.1 Hz), 3.15 (1H, d, J = 17.1 Hz), 3.22 (2H, m), 3.35 (1H, dd, J = 6.2, 7.4 Hz), 7.17–7.21 (3H, m), 7.24–7.29 (2H, m), 8.02 (1H, dd, J = 5.7, 5.7 Hz). ^{13}C NMR (DMSO-d_6, δ ppm): 33.6, 34.4, 38.6, 48.4, 62.2, 126.2, 128.0, 129.1, 137.7, 171.9, 172.0, 172.8. HRMS (ESI, negative): calcd for $C_{14}H_{18}N_2O_5$ $[M-H]^-$ 294.11430, found 294.11424.

5.1.2. *N*-(*tert*-Butoxycarbonyl)-L-4,4′-biphenylalanyl-β-alanine benzyl ester (8)

To a solution of Boc-3-(4-biphenylyl)-L-alanine (2.03 g, 5.95 mmol) in DMF (82 mL) were added HOBt anhydrous (1.61 g, 11.9 mmol), 4-methylmorpholine (NMM) (0.72 mL, 6.55 mmol), and β-alanine benzyl ester *p*-toluenesulfonate (**7**) (2.09 g, 5.95 mmol) under Ar atmosphere at room temperature and was added 1-ethyl-3-(3-dimethylaminopropyl)carbodiimide hydrochloride (WSC·HCl) (1.25 g, 6.55 mmol) at 0 °C. The reaction mixture was stirred for 19 h at 0 °C to room temperature. The mixture was quenched into satd NH_4Cl aq (70 mL) and extracted with EtOAc (50 mL × 2). The organic layer was poured with satd $NaHCO_3$ aq (30 mL) and brine (80 mL), and dried over $MgSO_4$.

Table 3
The calculated intermolecular energies and the inhibitory activities of compounds **1**–**6** against human NEP

Compounds	Structure	Intermolecular energy (kcal/mol)	IC_{50} (nM)
1	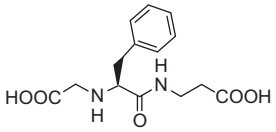	−15.17	44000
2	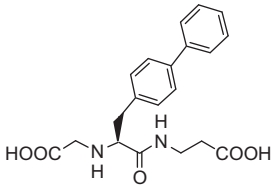	−17.32	9.7
3	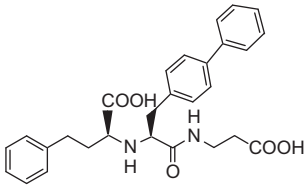	−19.30	0.36
4	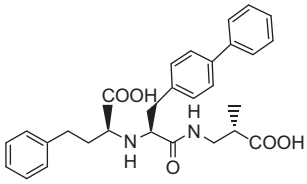	−17.85	0.51
5	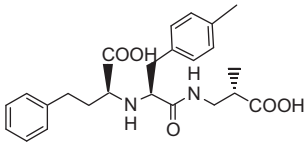	−15.47	430
6	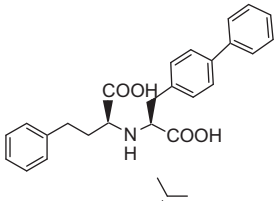	−15.23	420
Phospho-ramidon	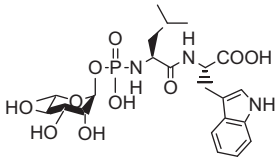	NC[a]	2.0

[a] Not calculated.

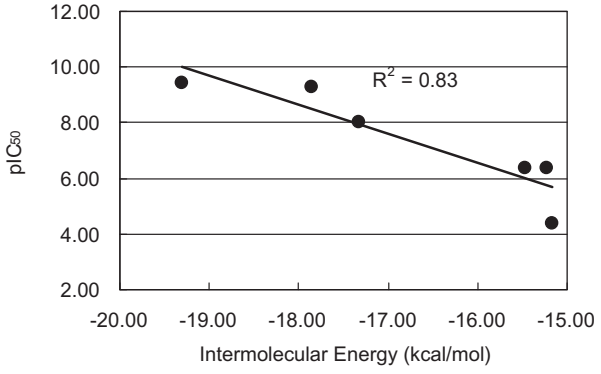

Figure 5. The correlation between the calculated interaction energies and the IC_{50} values of compounds **1**–**6**. pIC_{50} means $-\log(IC_{50})$.

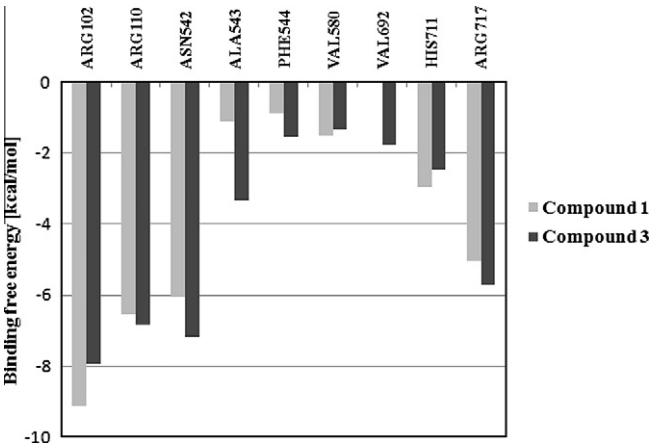

Figure 6. The decomposition analysis of binding free energies for individual hot spot amino acid residues of compound **1** or **3**.

The solvent was removed under reduced pressure and the residue was purified by silica gel flash chromatography using a gradient of EtOAc and *n*-hexane (0:100–50:50) as eluting solvent to give **8** (2.79 g, 93% yield) as white solid. mp: 109.1–109.8 °C. IR (ATR, cm^{-1}) ν 3313, 2977, 2933, 1732, 1655, 1520, 1166, 758, 697. ^1H NMR ($CDCl_3$, δ ppm): 1.42 (9H, s), 2.37–2.58 (2H, m), 3.04 (1H, dd, J = 7.5, 13.2 Hz), 3.00–3.15 (1H, m), 3.37–3.47 (1H, m), 3.52 (1H, dddd, J = 5.2, 6.8, 6.8, 13.6 Hz), 4.25–4.37 (1H, m), 4.95 (1H, d, J = 12.2 Hz), 5.03 (1H, d, J = 12.2 Hz), 6.23–6.35 (1H, m), 7.22–7.28 (5H, m), 7.30–7.36 (3H, m), 7.40–7.44 (2H, m), 7.52 (2H, dd, J = 2.0, 8.2 Hz), 7.55–7.58 (2H, m). ^{13}C NMR ($CDCl_3$, δ ppm): 28.3, 33.8, 34.7, 38.4, 55.9, 66.5, 80.2, 127.0, 127.30, 127.32, 128.2, 128.4, 128.6, 128.8, 129.7, 135.5, 135.7, 139.8, 140.6, 155.3, 171.0, 172.0.

5.1.3. L-4,4′-Biphenylalanyl-β-alanine benzyl ester hydrochloride (9)

Compound **8** (2.03 g, 4.05 mmol) was dissolved in 4 N HCl in 1,4-dioxane (10 mL) at room temperature and stirred for 1.5 h. The solvent was removed under reduced pressure and the residue was purified by silica gel flash chromatography using a gradient of MeOH and $CHCl_3$ (2:98–17:83) as eluting solvent to give **9** (1.69 g, 95% yield) as white solid. mp: 137.0–138.1 °C. IR (ATR, cm^{-1}) ν 3345, 3029, 2938, 2875, 1733, 1661, 1558, 1174, 759, 731, 695. ^1H NMR ($CDCl_3$, δ ppm): 2.34 (1H, ddd, J = 6.1, 6.1, 16.8 Hz), 2.36 (1H, ddd, J = 6.4, 6.4, 16.8 Hz), 3.27 (1H, dd, J = 7.9, 13.5 Hz), 3.29–3.40 (2H, m), 3.50 (1H, dddd, J = 5.7, 6.1, 6.4, 13.1 Hz), 4.37 (1H, m), 4.89 (1H, d, J = 12.3 Hz), 4.96 (1H, d, J = 12.3 Hz), 7.15–7.22 (2H, m), 7.22–7.30 (4H, m), 7.30–7.37 (4H, m), 7.42–7.50 (4H, m), 7.67 (1H, dd, J = 5.7, 5.7 Hz). ^{13}C NMR ($CDCl_3$, δ ppm): 33.7, 35.0, 37.9, 55.2, 66.5, 126.9, 127.28, 127.34, 128.19, 128.22, 128.5, 128.8, 130.1, 134.4, 135.5, 140.0, 140.4, 169.7, 171.9.

5.1.4. *N*-(Benzyloxycarbonylmethyl)-L-4,4′-biphenylalanyl-β-alanine benzyl ester (10)

To a solution of benzyl bromoacetate (1.25 mL, 7.89 mmol) and **9** (1.56 g, 3.57 mmol) in THF (32 mL) was added Et_3N (2.50 mL, 17.8 mmol) in THF (12 mL) under Ar atmosphere at room temperature and stirred for 29 h. The solvent was removed under reduced pressure and extracted with EtOAc (75 mL × 2). The organic layer was poured with satd $NaHCO_3$ aq and brine (80 mL), and dried over $MgSO_4$. The solvent was removed under reduced pressure and the residue was purified by silica gel flash chromatography using a gradient of EtOAc and *n*-hexane (35:65–66:34) as eluting solvent to give **10** (1.82 g, 93% yield) as pale yellow oil.

IR (ATR, cm^{-1}) ν 3335, 3032, 2951, 1736, 1670, 1520, 1174, 753, 737, 698. ^1H NMR ($CDCl_3$, δ ppm): 1.92 (1H, br s), 2.53 (1H, ddd, J = 5.9, 6.4, 16.9 Hz), 2.57 (1H, ddd, J = 5.7, 6.3, 16.9 Hz), 2.83 (1H, dd, J = 8.6, 13.8 Hz), 3.18 (1H, dd, J = 4.5, 13.8 Hz), 3.23 (1H, d, J = 17.7 Hz), 3.35 (1H, d, J = 17.7 Hz), 3.38 (1H, dd, J = 4.5, 8.6 Hz), 3.48–3.57 (2H, m), 5.04 (1H, d, J = 12.2 Hz), 5.07 (1H, d, J = 12.2 Hz), 5.08 (1H, d, J = 12.4 Hz), 5.10 (1H, d, J = 12.4 Hz), 7.26–7.36 (13H, m), 7.41–7.45 (2H, m), 7.51–7.55 (3H, m), 7.56–7.59 (2H, m). ^{13}C NMR ($CDCl_3$, δ ppm): 34.2, 34.5, 49.6, 63.6, 66.5, 66.8, 127.0, 127.27, 127.34, 128.4, 128.5, 128.59, 128.63, 128.8, 129.7, 135.3, 135.6, 136.0, 140.7, 171.5, 172.0, 173.0.

5.1.5. *N*-(Carboxymethyl)-L-4,4′-biphenylalanyl-β-alanine (2)

To a solution of **10** (873 mg 1.58 mmol) in MeOH (26 mL) was added 10% Pd/C (89.2 mg, 10 wt %) and vigorously stirred at room temperature for 3.5 h under hydrogen pressure (balloon). After removing the Pd/C by filtration, the filtrate was concentrated under reduced pressure and the residue was recrystallized from 40% MeOH aq to give **2** (230 mg, 39% yield) as white crystals.

UFLC: 97% purity. mp: 208.0–209.7 °C (dec.). IR (ATR, cm^{-1}) ν 3335, 2913, 1730, 1666, 1606, 1542, 1373, 1190, 766, 699, 673. ^1H NMR (DMSO-d_6, δ ppm): 2.32 (1H, ddd, J = 6.9, 6.9, 16.4 Hz), 2.35 (1H, ddd, J = 6.8, 6.8, 16.4 Hz), 2.81 (1H, dd, J = 7.3, 13.6 Hz), 2.91 (1H, dd, J = 6.2, 13.6 Hz), 3.09 (1H, d, J = 17.1 Hz), 3.18 (1H, d, J = 17.1 Hz), 3.20–3.30 (2H, m), 3.38 (1H, dd, J = 6.2, 7.2 Hz), 7.26–7.30 (2H, m), 7.35 (1H, ddd, J = 1.1, 1.1, 7.4 Hz), 7.43–7.47 (2H, m), 7.55–7.59 (2H, m), 7.63–7.67 (2H, m), 8.06 (1H, dd, J = 5.7, 5.7 Hz). ^{13}C NMR (DMSO-d_6, δ ppm): 33.7, 34.4, 38.2, 48.4, 62.2, 126.3, 126.4, 127.1, 128.8, 129.7, 137.1, 138.0, 139.9, 172.0, 172.1, 172.8. HRMS (ESI, positive): calcd for $C_{20}H_{22}N_2O_5$ $[M+H]^+$ 371.16015, found 371.16033.

5.1.6. *N*-(*tert*-Butoxycarbonyl)-α-(*S*)-methyl-β-alanine benzyl ester (12)

To a solution of (*S*)-3-(Boc-amino)-2-methylpropionic acid (**11**) (2.00 g, 9.84 mmol) in $CHCl_3$ (40 mL) were added BnOH (1.20 mL, 11.8 mmol), 4-dimethylaminopyridine (DMAP) (0.121 g, 0.992 mmol), and WSC·HCl (2.08 g, 10.8 mmol) under Ar atmosphere at 0 °C. The reaction mixture was stirred at 0 °C to room temperature for 6 h. The mixture was quenched into satd NH_4Cl aq (50 mL) and extracted with $CHCl_3$ (50 mL × 2). The organic layer was poured with satd $NaHCO_3$ aq (50 mL) and brine (50 mL), and dried over $MgSO_4$. The solvent was removed under reduced pressure and the residue was purified by silica gel flash chromatography using a gradient of EtOAc and *n*-hexane (0:100–50:50) as eluting solvent to give **12** (2.84 g, 98% yield) as colorless oil.

IR (ATR, cm^{-1}) ν 2978, 1715, 1506, 1171, 732, 698. ^1H NMR ($CDCl_3$, δ ppm): 1.19 (3H, d, J = 7.3 Hz), 1.43 (9H, s), 2.70–2.78 (1H, m), 3.25 (1H, ddd, J = 6.0, 8.0, 13.6 Hz), 3.35 (1H, ddd,, J = 4.9, 6.8, 13.6 Hz), 4.86–4.96 (1H, m), 5.13 (1H, d, J = 13.1 Hz), 5.15 (1H, d, J = 13.1 Hz), 7.32–7.39 (5H, m). ^{13}C NMR ($CDCl_3$, δ ppm): 14.7, 28.4, 40.1, 43.0, 66.4, 79.3, 128.0, 128.3, 128.6, 135.8, 155.9, 175.3.

5.1.7. α-(*S*)-Methyl-β-alanine benzyl ester hydrochloride (13)

Compound **12** (2.72 g, 9.27 mmol) was dissolved in 4 N HCl in 1,4-dioxane (14 mL) at room temperature and stirred for 1 h. The solvent was removed under reduced pressure and the residue was purified by silica gel flash chromatography using a gradient of MeOH and $CHCl_3$ (0:100–16:84) as eluting solvent to give **13** (1.97 g, 92% yield) as pale yellow solid. mp: 74.8–78.5 °C. IR (ATR, cm^{-1}) ν 3414, 2977, 1727, 1608, 749, 698. ^1H NMR (CD_3OD, δ ppm): 1.27 (3H, d, J = 7.3 Hz), 2.87 (1H, qdd, J = 5.1, 7.3, 8.4 Hz), 3.02 (1H, dd, J = 5.1, 12.9 Hz), 3.18 (1H, dd, J = 8.4, 12.9 Hz), 5.17 (1H, d, J = 12.3 Hz), 5.22 (1H, d, J = 12.3 Hz), 7.31–7.41 (5H, m). ^{13}C NMR (CD_3OD, δ ppm): 15.2, 39.0, 42.7, 68.1, 129.4, 129.5, 129.7, 137.2, 174.9.

5.1.8. *N*-(*tert*-Butoxycarbonyl)-L-4,4′-biphenylalanyl-α-(*S*)-methyl-β-alanine benzyl ester (14)

To a solution of Boc-3-(4-biphenylyl)-L-alanine (1.47 g, 4.31 mmol) in DMF (30 mL) were added HOBt anhydrous (1.17 g, 8.66 mmol), NMM (0.52 mL, 4.73 mmol), and **13** (0.988 g, 4.30 mmol) under Ar atmosphere at room temperature and was added WSC·HCl (0.912 g, 4.76 mmol) at 0 °C. The reaction mixture was stirred for 14 h at 0 °C to room temperature. The mixture was quenched into satd NH_4Cl aq (30 mL) and extracted with EtOAc (50 mL × 3). The organic layer was poured with satd $NaHCO_3$ aq (60 mL) and brine (50 mL), and dried over $MgSO_4$. The solvent was removed under reduced pressure and the residue was purified by silica gel flash chromatography using a gradient of EtOAc and *n*-hexane (0:100–50:50) as eluting solvent to give **14** (1.69 g, 76% yield) as white solid. mp: 129.3–130.1 °C. IR (ATR, cm^{-1}) ν 3316, 2977, 2936, 1732, 1656, 1520, 1169, 761, 697. ^1H NMR ($CDCl_3$, δ ppm): 1.09 (3H, d, J = 6.9 Hz), 1.41 (9H, s), 2.64–2.73 (1H, m), 3.06 (2H, d, J = 6.4 Hz), 3.31 (1H, ddd, J = 6.0, 7.7, 13.6 Hz), 3.29–3.39 (1H, m), 4.25–4.37 (1H, m), 4.91–4.99 (1H, m), 5.02 (1H, d, J = 12.3 Hz), 5.07 (1H, d, J = 12.3 Hz), 6.20–6.30 (1H, m), 7.22–7.29 (5H, m), 7.30–7.36 (3H, m), 7.41–7.45 (2H, m), 7.52 (2H, ddd, J = 2.1, 2.1, 8.3 Hz), 7.55–7.58 (2H, m). ^{13}C NMR ($CDCl_3$, δ ppm): 14.7, 28.3, 38.2, 39.3, 41.5, 55.9, 66.4, 80.2, 127.0, 127.3, 127.4, 128.1, 128.3, 128.6, 128.8, 129.7, 135.6, 135.7, 139.9, 140.7, 155.3, 171.2, 174.9.

Prepared similarly was the following compound.

5.1.9. *N*-(*tert*-Butoxycarbonyl)-L-4-methylphenylalanyl-α-(*S*)-methyl-β-alanine benzyl ester (15)

White solid, yield 96%. mp: 101.0–101.8 °C. IR (ATR, cm^{-1}) ν 3306, 2978, 2934, 1731, 1657, 1516, 1170, 752, 698. ^1H NMR ($CDCl_3$, δ ppm): 1.10 (3H, d, J = 7.1 Hz), 1.40 (9H, s), 2.30 (3H, s), 2.64–2.71 (1H, m), 2.92–3.02 (2H, m), 3.28 (1H, ddd, J = 6.0, 7.8, 13.7 Hz), 3.36–3.48 (1H, m), 4.15–4.30 (1H, m), 4.85–5.00 (1H, m), 5.06 (1H, d, J = 12.3 Hz), 5.11 (1H, d, J = 12.3 Hz), 6.12–6.25 (1H, m), 7.05 (2H, d, J = 7.9 Hz), 7.09 (2H, d, J = 7.9 Hz), 7.30–7.39 (5H, m). ^{13}C NMR ($CDCl_3$, δ ppm): 14.7, 21.0, 28.3, 38.1, 39.3, 41.4, 55.9, 66.4, 80.1, 128.1, 128.4, 128.6, 129.1, 129.4, 133.4, 135.7, 136.5, 155.3, 171.4, 174.9.

5.1.10. L-4,4′-Biphenylalanyl-β-alanine benzyl ester formate (16a)

Compound **8** (1.41 g, 2.80 mmol) was dissolved in HCOOH (14 mL) at room temperature and stirred for 16 h. The solvent was removed under reduced pressure and the residue was purified by silica gel flash chromatography using a gradient of MeOH and $CHCl_3$ (0:100–17:83) as eluting solvent to give **16a** (0.947 g, 75% yield) as white solid. mp: 116.3–117.5 °C. IR (ATR, cm^{-1}) ν 3295, 3031, 2948, 1732, 1661, 1521, 1173, 761, 697. ^1H NMR ($CDCl_3$, δ ppm): 2.51–2.60 (2H, m), 2.82 (1H, dd, J = 8.6, 13.7 Hz), 3.22 (1H, dd, J = 5.2, 13.7 Hz), 3.49–3.58 (2H, m), 3.72 (3H, br s), 3.74 (1H, dd, J = 5.2, 8.6 Hz), 5.06 (1H, d, J = 12.3 Hz), 5.08 (1H, d, J = 12.3 Hz), 7.25–7.36 (8H, m), 7.41–7.45 (2H, m), 7.51–7.59 (5H, m), 8.10 (1H, br s). ^{13}C NMR ($CDCl_3$, δ ppm): 34.0, 34.7, 40.1, 56.0, 66.6, 127.0, 127.3, 127.5, 128.3, 128.4, 128.6, 128.8, 129.7, 135.5, 136.1, 140.0, 140.6, 164.1, 172.1, 173.4.

Prepared similarly were the following compounds.

5.1.11. L-4,4′-Biphenylalanyl-α-(*S*)-methyl-β-alanine benzyl ester formate (16b)

White solid, yield 99%. mp: 108.0–109.1 °C. IR (ATR, cm^{-1}) ν 3251, 3030, 2940, 1729, 1664, 1561, 1523, 1176, 761, 733, 696. ^1H NMR ($CDCl_3$, δ ppm): 1.11 (3H, d, J = 7.1 Hz), 2.69 (1H, m),

2.89 (1H, dd, J = 7.8, 13.6 Hz), 3.18 (1H, dd, J = 5.4, 13.6 Hz), 3.36 (1H, ddd, J = 6.0, 7.5, 13.6 Hz), 3.40–3.47 (1H, m), 3.81–3.92 (1H, m), 4.80 (3H, br s), 5.06 (1H, d, J = 12.3 Hz), 5.09 (1H, d, J = 12.3 Hz), 7.24–7.36 (8H, m), 7.40–7.44 (2H, m), 7.47 (1H, dd, J = 5.7, 6.0 Hz), 7.51–7.58 (4H, m), 8.15 (1H, br s). ^{13}C NMR ($CDCl_3$, δ ppm): 14.8, 39.3, 39.5, 41.6, 55.7, 66.5, 127.0, 127.4, 127.5, 128.2, 128.3, 128.6, 128.8, 129.8, 135.3, 135.7, 140.1, 140.5, 165.5, 172.4, 174.9.

5.1.12. L-4-Methylphenylalanyl-α-(*S*)-methyl-β-alanine benzyl ester formate (16c)

Pale yellow oil, yield 96%. IR (ATR, cm^{-1}) ν 3280, 2977, 2938, 1731, 1644, 1561, 1516, 1176, 753, 698. ^{1}H NMR ($CDCl_3$, δ ppm): 1.14 (3H, d, J = 7.3 Hz), 2.31 (3H, s), 2.70 (1H, qdd, J = 5.2, 7.3, 8.0 Hz), 2.74 (1H, dd, J = 8.3, 13.8 Hz), 3.11 (1H, dd, J = 5.6, 13.8 Hz), 3.34 (1H, ddd, J = 5.8, 8.0, 13.6 Hz), 3.46 (1H, ddd, J = 5.2, 6.6, 13.6 Hz), 3.75 (1H, dd, J = 5.6, 8.3 Hz), 4.02 (3H, br s), 5.10 (1H, d, J = 12.3 Hz), 5.13 (1H, d, J = 12.3 Hz), 7.07 (2H, d, J = 7.9 Hz), 7.11 (2H, d, J = 7.9 Hz), 7.30–7.41 (6H, m), 8.09 (1H, br s). ^{13}C NMR ($CDCl_3$, δ ppm): 14.8, 21.1, 39.5, 41.6, 55.8, 66.5, 128.2, 128.4, 128.6, 129.1, 129.5, 133.3, 135.7, 136.8, 164.6, 172.8, 174.9.

5.1.13. *N*-[1-(*S*)-Benzyloxycarbonyl-3-phenylpropyl]-L-4,4′-biphenylalanyl-β-alanine benzyl ester (17a)

To a solution of (*R*)-2-hydroxy-4-phenylbutyric acid benzyl ester (1.11 g, 4.09 mmol) in CH_2Cl_2 (28 mL) were added Et_3N (1.30 mL, 9.33 mmol) and trifluoromethanesulfonic anhydride (Tf_2O) (0.77 mL, 4.69 mmol) under Ar atmosphere at −78 °C and stirred for 1 h. To the solution was added a solution of **16a** (0.835 g, 1.86 mmol) and Et_3N (0.28 mL, 2.01 mmol) in CH_2Cl_2 (10 mL) under Ar atmosphere at −78 °C. The reaction mixture was stirred at −78 °C to room temperature for 3 days. The solvent was removed under reduced pressure and extracted with EtOAc (30 mL × 3). The organic layer was poured with brine (50 mL) and dried over $MgSO_4$. The solvent was removed under reduced pressure and the residue was purified by silica gel flash chromatography using a gradient of EtOAc and *n*-hexane (0:100–50:50) as eluting solvent to give **17a** (0.982 g, 81% yield) as yellow oil.

IR (ATR, cm^{-1}) ν 3378, 3030, 2950, 1732, 1672, 1518, 1171, 752, 733, 698. ^{1}H NMR ($CDCl_3$, δ ppm): 1.76–1.86 (1H, m), 1.86–2.00 (1H, m), 1.98 (1H, br s), 2.50 (1H, t, J = 6.1 Hz), 2.53 (1H, dd, J = 6.0, 10.2, 13.8 Hz), 2.62 (1H, ddd, J = 6.0, 10.1, 14.2 Hz), 2.86 (1H, dd, J = 8.0, 13.7 Hz), 3.09 (1H, dd, J = 4.4, 13.7 Hz), 3.18 (1H, dd, J = 5.7, 5.7 Hz), 3.43 (1H, dd, J = 4.4, 8.0 Hz), 3.48 (2H, td, J = 6.1, 6.1 Hz), 4.97 (1H, d, J = 12.1 Hz), 5.01 (2H, s), 5.07 (1H, d, J = 12.1 Hz), 7.05–7.09 (2H, m), 7.15 (1H, ddd, J = 1.3, 1.3, 8.6 Hz), 7.21–7.36 (15H, m), 7.40–7.45 (2H, m), 7.48–7.54 (3H, m), 7.56–7.59 (2H, m). ^{13}C NMR ($CDCl_3$, δ ppm): 31.8, 34.1, 34.3, 35.1, 39.3, 60.2, 62.4, 66.7, 126.1, 127.0, 127.20, 127.24, 128.2, 128.30, 128.33, 128.4, 128.47, 128.48, 128.57, 128.63, 128.8, 129.8, 135.4, 135.5, 135.7, 139.8, 140.7, 140.8, 172.1, 173.1, 174.0.

Prepared similarly were the following compounds.

5.1.14. *N*-[1-(*S*)-Benzyloxycarbonyl-3-phenylpropyl]-L-4,4′-biphenylalanyl-α-(*S*)-methyl-β-alanine benzyl ester (17b)

Yellow oil, yield 62%. IR (ATR, cm^{-1}) ν 3361, 3029, 2936, 1730, 1672, 1517, 1172, 751, 736, 697. ^{1}H NMR ($CDCl_3$, δ ppm): 1.16 (1H, d, J = 7.3 Hz), 1.75–1.83 (1H, m), 1.85–1.97 (1H, m), 1.95 (1H, br s), 2.52 (1H, ddd, J = 6.0, 10.2, 14.0 Hz), 2.60 (1H, ddd, J = 5.9, 10.1, 14.0 Hz), 2.68 (1H, qdd, J = 4.6, 7.3, 8.2 Hz), 2.81 (1H, dd, J = 8.1, 13.9 Hz), 3.07 (1H, dd, J = 4.5, 13.9 Hz), 3.14–3.22 (1H, m), 3.30 (1H, ddd, J = 5.8, 8.2, 13.7 Hz), 3.33 (1H, dd, J = 4.5, 8.1 Hz), 3.47 (1H, ddd, J = 4.6, 7.0, 13.7 Hz), 4.96 (1H, d, J = 12.1 Hz), 4.99 (1H, d, J = 12.3 Hz), 5.06 (1H, d, J = 12.1 Hz), 5.07 (1H, d, J = 12.3 Hz), 7.04–7.07 (2H, m), 7.16 (1H, ddd, J = 1.1, 1.1, 7.4 Hz), 7.20–7.36 (15H, m), 7.39–7.45 (2H, m), 7.46 (1H, dd, J = 5.8, 7.0 Hz), 7.50–7.54 (2H, m), 7.56–7.59 (2H, m). ^{13}C NMR ($CDCl_3$, δ ppm): 15.0, 31.8, 35.2, 39.3, 39.6, 41.1, 60.3, 62.4, 66.4, 66.7, 126.1, 127.0, 127.20, 127.22, 128.0, 128.25, 128.29, 128.4, 128.5, 128.57, 128.62, 128.8, 129.8, 135.4, 135.7, 139.7, 140.7, 140.8, 173.2, 174.0, 174.9.

5.1.15. *N*-[1-(*S*)-Benzyloxycarbonyl-3-phenylpropyl]-L-4-methylphenylalanyl-α-(*S*)-methyl-β-alanine benzyl ester (17c)

Yellow oil, yield 57%. IR (ATR, cm^{-1}) ν 3377, 3029, 2936, 1731, 1673, 1514, 1172, 749, 698. ^{1}H NMR ($CDCl_3$, δ ppm): 1.16 (3H, d, J = 7.3 Hz), 1.72–1.81 (1H, m), 1.83–2.00 (1H, m), 1.92 (1H, br s), 2.30 (3H, s), 2.50 (1H, ddd, J = 5.9, 10.4, 13.9 Hz), 2.59 (1H, ddd, J = 5.9, 10.5, 13.9 Hz), 2.64–2.72 (2H, m), 3.01 (1H, dd, J = 4.4, 13.9 Hz), 3.16 (1H, dd, J = 6.8, 6.9 Hz), 3.27 (1H, dd, J = 4.4, 8.7 Hz), 3.30 (1H, ddd, J = 5.9, 8.0, 13.7 Hz), 3.46 (1H, ddd, J = 4.7, 7.0, 13.7 Hz), 4.94 (1H, d, J = 12.1 Hz), 5.05 (1H, d, J = 12.1 Hz), 5.06 (1H, d, J = 12.4 Hz), 5.09 (1H, d, J = 12.4 Hz), 7.01–7.06 (4H, m), 7.07–7.10 (2H, m), 7.16 (1H, ddd, J = 1.3, 1.3, 7.4 Hz), 7.20–7.25 (2H, m), 7.25–7.38 (10H, m), 7.43 (1H, dd, J = 4.7, 5.9 Hz). ^{13}C NMR ($CDCl_3$, δ ppm): 14.9, 21.1, 31.8, 35.2, 39.3, 39.6, 41.1, 60.2, 62.5, 66.4, 66.7, 126.1, 128.0, 128.3, 128.4, 128.5, 128.60, 128.61, 129.2, 129.3, 133.5, 135.4, 135.8, 136.4, 140.8, 173.4, 174.0, 174.9.

5.1.16. *N*-[1-(*S*)-Carboxy-3-phenylpropyl]-L-4,4′-biphenylalanyl-β-alanine (3)

To a solution of **17a** (0.894 g, 1.36 mmol) in DMF (27 mL) was added 10% Pd/C (90.6 mg) and vigorously stirred at room temperature for 23 h under hydrogen pressure (balloon). After removing the Pd/C by filtration, the filtrate was concentrated under reduced pressure. The residue was again dissolved in DMF (26 mL). To a solution was added 10% Pd/C (91.4 mg) and vigorously stirred at room temperature for 14.5 h under hydrogen pressure (balloon). After removing the Pd/C by filtration, the filtrate was concentrated under reduced pressure. The residue was recrystallized from 80% DMF aq to give **3** (0.164 g, 25% yield) as white crystals.

UFLC: >99% purity. mp: 225.5–227.0 °C (dec.). IR (ATR, cm^{-1}) ν 3369, 3030, 2880, 1725, 1677, 1612, 1533, 1391, 1192, 760, 751, 703, 694. ^{1}H NMR (DMSO-d_6, δ ppm): 1.73–1.85 (2H, m), 2.30 (2H, dd, J = 6.9, 6.9 Hz), 2.62 (2H, dd, J = 8.0, 8.0 Hz), 2.85 (1H, dd, J = 7.0, 13.6 Hz), 2.89 (1H, dd, J = 6.2, 13.6 Hz), 3.02 (1H, dd, J = 5.8, 6.9 Hz), 3.18–3.30 (2H, m), 3.31 (1H, dd, J = 6.2, 7.0 Hz), 7.15–7.20 (3H, m), 7.24–7.29 (4H, m), 7.35 (1H, ddd, J = 1.2, 1.2, 7.3 Hz), 7.43–7.47 (2H, m), 7.55–7.59 (2H, m), 7.63–7.67 (2H, m), 7.89 (1H, dd, J = 5.9, 5.9 Hz). ^{13}C NMR (DMSO-d_6, δ ppm): 31.2, 33.6, 34.3, 34.4, 38.6, 58.9, 61.9, 125.7, 126.3, 126.4, 127.1, 128.16, 128.17, 128.8, 129.7, 136.8, 138.0, 139.9, 141.5, 172.1, 172.9, 175.0. HRMS (ESI, positive): calcd for $C_{28}H_{30}N_2O_5$ $[M+H]^+$ 475.2228, found 475.2222.

Prepared similarly was the following compound.

5.1.17. *N*-[1-(*S*)-Carboxy-3-phenylpropyl]-L-4,4′-biphenylalanyl-α-(*S*)-methyl-β-alanine (4)

White crystals (recrystallization from 90% DMF aq), yield 37%. UFLC: >99% purity. mp: 243.0–243.8 °C (dec.). IR (ATR, cm^{-1}) ν 3384, 3031, 2925, 1725, 1678, 1615, 1530, 1359, 1203, 757, 732, 703, 692. ^{1}H NMR (DMSO-d_6, δ ppm): 0.90 (3H, d, J = 7.1 Hz), 1.74–1.86 (2H, m), 2.42 (1H, qdd, J = 6.3, 6.3, 7.1 Hz), 2.62 (2H, dd, J = 8.1, 8.1 Hz), 2.86 (1H, dd, J = 7.0, 13.6 Hz), 2.90 (1H, dd, J = 6.6, 13.6 Hz), 3.02 (1H, ddd, J = 6.0, 6.3, 13.1 Hz), 3.05 (1H, dd, J = 5.9, 6.7 Hz), 3.30 (1H, ddd, J = 6.0, 6.3, 13.1 Hz), 3.35 (1H, dd, J = 6.6, 7.0 Hz), 7.14–7.20 (3H, m), 7.23–7.29 (4H, m), 7.33–7.37 (1H, m), 7.43–7.48 (2H, m), 7.54–7.59 (2H, m), 7.62–7.66 (2H, m), 7.90 (1H, dd, J = 6.0, 6.0 Hz). ^{13}C NMR (DMSO-d_6, δ ppm): 14.5, 31.2, 34.5, 38.68, 38.70, 40.8, 59.0, 61.9, 125.7, 126.3, 126.4,

127.1, 128.2, 128.8, 129.7, 136.8, 138.0, 139.9, 141.4, 172.2, 174.9, 175.9. HRMS (ESI, positive): calcd for $C_{29}H_{32}N_2O_5$ $[M+H]^+$ 489.2384, found 489.2377.

Prepared similarly using AcOH:MeOH:H_2O (6:3:1) as solvent instead of DMF was the following compound.

5.1.18. *N*-[1-(*S*)-Carboxy-3-phenylpropyl]-L-4-methylphenylalanyl-α-(*S*)-methyl-β-alanine (5)

White crystals (recrystallization from 50% DMF aq), yield 46%. UFLC: >99% purity. mp: 200.2–201.2 °C (dec.). IR (ATR, cm^{-1}) *ν* 3383, 3025, 2906, 1733, 1678, 1612, 1537, 1361, 1193, 773, 745, 698. ^{1}H NMR (DMSO-d_6, *δ* ppm): 0.92 (3H, d, *J* = 7.2 Hz), 1.71–1.84 (2H, m), 2.26 (3H, s), 2.41 (1H, qdd, *J* = 6.9, 7.2, 7.2 Hz), 2.60 (2H, t, *J* = 8.0 Hz), 2.75 (1H, dd, *J* = 7.2, 13.5 Hz), 2.81 (1H, dd, *J* = 6.2, 13.5 Hz), 2.97–3.05 (1H, m), 3.01 (1H, dd, *J* = 6.5, 6.5 Hz), 3.23–3.30 (1H, m), 3.27 (1H, dd, *J* = 6.2, 7.2 Hz), 7.04–7.08 (4H, m), 7.14–7.20 (3H, m), 7.23–7.29 (2H, m), 7.84 (1H, dd, *J* = 6.2, 6.3 Hz). ^{13}C NMR (DMSO-d_6, *δ* ppm): 14.5, 20.6, 31.2, 34.4, 38.6, 38.7, 40.8, 59.0, 62.0, 125.7, 128.2, 128.6, 128.9, 134.2, 135.1, 141.4, 172.2, 174.8, 175.9(ppm). HRMS (ESI, positive): calcd for $C_{24}H_{30}N_2O_5$ $[M+H]^+$ 427.2227, found 427.2222.

5.1.19. *N*-(*tert*-Butoxycarbonyl)-L-4,4′-biphenylalanine benzyl ester (19)

To a solution of Boc-L-4,4′-biphenylalanine (**18**) (1.99 g, 5.84 mmol) in $CHCl_3$ (40 mL) were added BnOH (0.78 mL, 7.53 mmol), DMAP (0.0721 g, 0.590 mmol), and WSC·HCl (1.23 g, 6.42 mmol) under Ar atmosphere at 0 °C. The reaction mixture was stirred at 0 °C to room temperature for 2 h. The mixture was poured into H_2O (60 mL) and extracted with $CHCl_3$ (50 mL × 2). The organic layer was poured with satd $NaHCO_3$ aq (90 mL) and brine (50 mL), and dried over $MgSO_4$. The solvent was removed under reduced pressure and the residue was purified by silica gel flash chromatography using a gradient of EtOAc and *n*-hexane (4:96–25:75) as eluting solvent to give **19** (2.44 g, 97% yield) as white solid. mp: 99.1–99.3 °C. IR (ATR, cm^{-1}) *ν* 3373, 3030, 2976, 1741, 1712, 1488, 1161, 758, 697. ^{1}H NMR ($CDCl_3$, *δ* ppm): 1.42 (9H, s), 3.11 (1H, dd, *J* = 6.0, 13.9 Hz), 3.15 (1H, dd, *J* = 6.1, 13.9 Hz), 4.67 (1H, ddd, *J* = 6.0, 6.1, 8.2 Hz), 5.03 (1H, d, *J* = 8.1 Hz), 5.12 (1H, d, *J* = 12.2 Hz), 5.19 (1H, d, *J* = 12.2 Hz), 7.08–7.12 (2H, m), 7.28–7.36 (6H, m), 7.42–7.49 (4H, m), 7.54–7.57 (2H, m). ^{13}C NMR ($CDCl_3$, *δ* ppm): 28.3, 37.9, 54.4, 67.2, 80.0, 127.0, 127.22, 127.24, 128.5, 128.8, 129.8, 134.9, 135.1, 139.9, 140.7, 155.1, 171.7.

5.1.20. L-4, 4′-Biphenylalanine benzyl ester formate (20)

Compound **19** (2.18 g, 5.05 mmol) was dissolved in HCOOH (22 mL) at room temperature and stirred for 13 h. The solvent was removed under reduced pressure and the residue was purified by silica gel flash chromatography using a gradient of MeOH and $CHCl_3$ (0:100–9:91) as eluting solvent to give **20** (1.93 g, quant.) as white solid. mp: 100.5–102.0 °C. IR (ATR, cm^{-1}) *ν* 3030, 2760, 2681, 1743, 1563, 1557, 1347, 1224, 1206, 760, 741, 697, 691. ^{1}H NMR (CD_3OD, *δ* ppm): 3.19 (1H, dd, *J* = 6.9, 14.5 Hz), 3.22 (1H, dd, *J* = 7.1, 14.5 Hz), 4.31 (1H, dd, *J* = 6.9, 7.1 Hz), 5.20 (1H, d, *J* = 12.0 Hz), 5.25 (1H, d, *J* = 12.0 Hz), 7.22–7.26 (2H, m), 7.27–7.37 (6H, m), 7.41–7.46 (2H, m), 7.53–7.57 (2H, m), 7.57–7.61 (2H, m), 8.32 (1H, br s). ^{13}C NMR (CD_3OD, *δ* ppm): 37.7, 55.4, 69.1, 127.9, 128.60, 128.63, 129.7, 129.8, 130.0, 131.0, 134.6, 136.3, 141.8, 142.0, 167.6, 170.8.

5.1.21. *N*-[1-(*S*)-Benzyloxycarbonyl-3-phenylpropyl]-L-4,4′-biphenylalanine benzyl ester (21)

To a solution of (*R*)-2-hydroxy-4-phenylbutyric acid benzyl ester (1.86 g, 6.87 mmol) in CH_2Cl_2 (27 mL) were added Et_3N (2.30 mL, 16.5 mmol) and Tf_2O (1.30 mL, 7.73 mmol) under Ar atmosphere at −78 °C and stirred for 1.5 h. To the solution was added a solution of **20** (1.17 g, 3.11 mmol) and Et_3N (0.48 mL, 3.44 mmol) in CH_2Cl_2 (19 mL) under Ar atmosphere at −78 °C. The reaction mixture was stirred at −78 °C to room temperature for 3 days. The solvent was removed under reduced pressure and extracted with EtOAc (50 mL × 3). The organic layer was poured with brine (80 mL) and dried over $MgSO_4$. The solvent was removed under reduced pressure and the residue was purified by silica gel flash chromatography using a gradient of EtOAc and *n*-hexane (6:94–27:83) as eluting solvent to give **21** (0.800 g, 44% yield) as yellow oil.

IR (ATR, cm^{-1}) *ν* 3030, 2934, 1732, 1166, 753, 735, 697. ^{1}H NMR ($CDCl_3$, *δ* ppm): 1.87 (1H, dddd, *J* = 6.1, 6.9, 10.1, 13.4 Hz), 1.95 (1H, dddd, *J* = 6.1, 6.1, 10.1, 13.4 Hz), 2.56 (1H, ddd, *J* = 6.1, 10.1, 13.9 Hz), 2.61 (1H, ddd, *J* = 6.1, 10.1, 13.9 Hz), 2.97 (1H, dd, *J* = 7.2, 13.5 Hz), 3.04 (1H, dd, *J* = 7.2, 13.5 Hz), 3.38 (1H, dd, *J* = 6.1, 6.9 Hz), 3.67 (1H, dd, *J* = 7.2, 7.2 Hz), 5.01 (1H, d, *J* = 12.1 Hz), 5.06 (1H, d, *J* = 12.1 Hz), 5.07 (1H, d, *J* = 12.1 Hz), 5.09 (1H, d, *J* = 12.1 Hz), 7.05–7.09 (2H, m), 7.14–7.20 (5H, m), 7.21–7.36 (11H, m), 7.41–7.48 (4H, m), 7.54–7.58 (2H, m). ^{13}C NMR ($CDCl_3$, *δ* ppm): 31.8, 35.0, 39.4, 59.4, 61.1, 66.6, 66.7, 125.9, 127.0, 127.16, 127.20, 128.30, 128.33, 128.37, 128.41, 128.5, 128.3, 128.7, 129.6, 135.4, 135.6, 135.7, 139.7, 140.8, 141.2, 173.7, 174.1.

5.1.22. *N*-[1-(*S*)-Carboxy-3-phenylpropyl]-L-4,4′-biphenylalanine (6)

To a solution of **21** (555 mg, 0.951 mmol) in DMF (19 mL) was added 10% Pd/C (55.1 mg) and vigorously stirred at room temperature for 15.5 h under hydrogen pressure (balloon). After removing the Pd/C by filtration, the filtrate was concentrated under reduced pressure and the residue was recrystallized from 90% DMF aq to give **6** (105 mg, 27% yield) as white crystals.

UFLC: >99% purity. mp: 241.0–242.0 °C (dec.). IR (ATR, cm^{-1}) *ν* 3004, 2865, 1719, 1590, 1287, 1245, 761, 751, 701, 693. ^{1}H NMR (DMSO-d_6, *δ* ppm): 1.76 (1H, dddd, *J* = 5.9, 6.8, 9.5, 13.4 Hz), 1.83 (1H, dddd, *J* = 5.8, 6.6, 9.4, 13.4 Hz), 2.59 (1H, ddd, *J* = 5.9, 9.4, 13.8 Hz), 2.63 (1H, ddd, *J* = 6.6, 9.5, 13.8 Hz), 2.91 (1H, dd, *J* = 6.5, 13.6 Hz), 2.95 (1H, dd, *J* = 7.0, 13.6 Hz), 3.20 (1H, dd, *J* = 5.8, 6.8 Hz), 3.50 (1H, dd, *J* = 6.5, 7.0 Hz), 7.15–7.20 (3H, m), 7.24–7.28 (2H, m), 7.29–7.33 (2H, m), 7.33–7.37 (1H, m), 7.43–7.47 (2H, m), 7.56–7.60 (2H, m), 7.63–7.67 (2H, m). ^{13}C NMR (DMSO-d_6, *δ* ppm): 31.1, 34.5, 38.2, 58.4, 60.6, 125.7, 126.3, 126.4, 127.2, 128.18, 128.22, 128.8, 129.7, 136.9, 138.0, 139.8, 141.5, 174.3, 175.0. HRMS (ESI, positive): calcd for $C_{25}H_{25}NO_4$ $[M+H]^+$ 404.1856, found 404.1852.

5.2. Biological procedures

5.2.1. Preparation of human fibroblast homogenate

Normal human dermal fibroblasts, derived from neonatal foreskin (Kurabo, Japan), were cultivated in Dulbecco's Modified Eagle's Medium (DMEM) with 10% fetal calf serum (FCS) at 37 °C in 5% CO_2 atmosphere. Cultured fibroblasts were washed once with phosphate-buffered saline (PBS), scraped into PBS, and centrifuged at 4 °C, 15,000 rpm for 5 min. The cell pellets were suspended with 0.1% Triton X-100/0.2 M Tris–HCl, followed by ultrasonication on ice. Cleared supernatants after the removal of cell residues by centrifugation (15,000 rpm, 5 min, 4 °C) were diluted with the buffer, consisting of 0.1 M MES–NaOH (pH 6.5) and 0.3 M NaCl, and used as the fibroblast enzyme solution (protein concentration (BCA): ca. 30 μg/mL).

5.2.2. Enzyme assay

The activity of NEP using the synthetic substrate GAAP (glutaryl-Ala-Ala-Phe-4-methoxy-2-naphtylamide) was measured as

previously by MacDonald and co-workers.[15] In brief, 100 μL of enzyme solution was dispensed into 96-well plates and added to the compounds at different concentrations. After addition of 2 μL of 10 mM GAAP in DMF, the plates were incubated for 1 h at 37 °C. At the end of the incubation period, the NEP-catalyzed reaction was terminated by addition of 1 μL of 100 μM phosphoramidon in DMSO. After addition of 2 μL of 25 mU Leucine aminopeptidase M in H_2O (SIGMA, USA), the plates were further incubated for 1 h at 37 °C. The release of 4-methoxy-2-naphtylamine was measured by an excitation wavelength at 340 nm and an emission wavelength at 425 nm. Phosphoramidon was used as a positive control. From each compound **7** concentrations, the compounds serially diluted in half-log steps were tested in triplicates. The IC_{50} values were calculated using Graphpad Prism version 5.02 software.

5.3. Computational procedures

5.3.1. Molecular docking

The structure of NEP was obtained from the Protein Data Bank (code 2QPJ). Before docking, all the ligands and water molecules were removed from the PDB file. Molecular docking was carried out with the AutoDock4.2.[12] Approximate binding free energies calculated by this program are based on an empirical function, derived by linear regression analysis of protein–ligand complexes with known binding constants. The docking compatible structure formats of the NEP were prepared by AutoDockTools-1.5.4, an accessory program[12] that allows the user to interact with AutoDock 4.2 from a graphic user interface. The number of grid points in *xyz* was set to 40, 40, 40, the spacing value equivalent to 0.375 Å, and the grid center to 23.636, 48.243, 32.901. During docking studies, a Lamarckian Genetic Algorithm was utilized and energy evaluations were set at 5×10^5 on scaffold A optimization and 8×10^5 on scaffold B optimization, respectively. Each simulation was performed a total of 20 times. The default settings were used for all other parameters. In the case of scaffold B optimization, we defined Phe544 of the NEP as the flexible residue. The molecular docking was performed against the dipeptide derivatives derived from our in-house amino acid derivatives library and small and hydrophobic fragments library, respectively.

5.3.2. MM/GBSA free energy decomposition analysis

To identify hot spot amino acid residues in protein–ligand interfaces, the free energy decomposition analysis using the MM-GB/SA[19–21] was performed by *mm_pbsa module* of Amber 9.[22] The detailed description of MM-GB/SA decomposition procedure used in Amber was reported by Gohlke et al.[23] The free energy decomposition based on MM-GB/SA is a pragmatic way to estimate the contribution of each residue to protein-ligand interactions.

The MM-GB/SA approach employs molecular mechanics, the generalized Born model[24] and solvent accessibility method to elicit free energies from structural information.

$$\Delta G_{\text{bind}} = G_{\text{complex}} - G_{\text{protein}} - G_{\text{ligand}} = \Delta E_{\text{MM}} + \Delta G_{\text{GB}} + \Delta G_{\text{nonpolar}} - T\Delta S \quad (1)$$

The binding free energy (ΔG_{bind}) is calculated as the sum of the energetic contributions, which correspond to the molecular mechanical gas-phase energies ($\Delta E_{\text{MM}} = \Delta E_{\text{elec}} + \Delta E_{\text{vdw}}$) and the desolvation free energies ($\Delta G_{\text{GB}} + \Delta G_{\text{nonpolar}}$), plus the entropic contributions ($-T\Delta S$) which were not considered in this study because of the high computational cost. The desolvation free energies were estimated as the sum of an electrostatic desolvation energy (ΔG_{GB}), calculated with the generalized Born model,[24] plus a nonpolar desolvation energy ($\Delta G_{\text{nonpolar}}$).[23] NEP is a membrane-bound zinc metallopeptidase. The catalytic zinc ion is coordinated to three amino acid residues (His583, His587 and Glu646) at the active site. Because of considerations involved in the MM-GB/SA approach, the non-bonded model for the zinc ion ($q = +2e^-$, $R^* = 1.40$ Å, $\varepsilon = 0.01$ kcal/mol) was adopted.[25] The complex structure of dipeptide derivatives with the NEP was energy minimized by 100 steps of conjugate gradient minimization in implicit water model (GB/SA). The harmonic restraints with force constants of 300 kcal/mol Å^2 applied to a zinc and atoms of three amino acid residues (His583, His587 and Glu646) at the active site. In the MM-GB/SA calculation, the single energy-minimized complex structure was used.

Supplementary data

Supplementary data associated with this article can be found, in the online version, at doi:10.1016/j.bmc.2011.08.064. These data include MOL files and InChiKeys of the most important compounds described in this article.

References and notes

1. Kerr, M. A.; Kenny, A. J. *Biochem. J.* **1974**, *137*, 477.
2. Roques, R. P.; Noble, F.; Dauge, V.; Fournie-Zaluski, M.-C.; Beaumont, A. *Pharmacol. Rev.* **1993**, *45*, 87.
3. Erdos, E. G.; Skidgel, R. A. *FASEB J.* **1989**, *3*, 145.
4. Jandeleit-Dahm, K. A. M. *J. Hum. Hypertens.* **2006**, *20*, 478.
5. Morisaki, N.; Moriwaki, S.; Sugiyama-Nakagiri, Y.; Haketa, K.; Takema, Y.; Imokawa, G. *J. Biol. Chem.* **2010**, *285*, 39819.
6. Dive, V.; Chang, C.-F.; Yiotakis, A.; Sturrock, E. D. *Curr. Pharm. Des.* **2009**, *15*, 3606.
7. Thanawala, V.; Kadam, V. J.; Ghosh, R. *Curr. Drug Target* **2008**, *9*, 887.
8. Spyroulias, G. A.; Cordopatis, P. *Curr. Enzyme Inhib.* **2005**, *1*, 29.
9. Schwartz, J. C. *Int. J. Antimicrob. Agents* **2000**, *14*, 75.
10. Oefner, C.; D'Arcy, A.; Hennig, M.; Winkler, F. K.; Dale, G. E. *J. Mol. Biol.* **2000**, *296*, 341.
11. Watanabe, M.; Amano, S.; Suzuki, Y. JP 2,002,088,097, 2002.
12. Morris, G. M.; Huey, R.; Lindstrom, W.; Sanner, M. F.; Belew, R. K.; Goodsell, D. S.; Olson, A. J. *J. Comput. Chem.* **2009**, *30*, 2785.
13. Oefner, C.; Pierau, S.; Schulz, H.; Dale, G. E. *Acta Crystallogr.* **2007**, *D63*, 975.
14. Valles, R. M. WO 9,923,064, 1999.
15. Casey, M. L.; Smith, J. W.; Nagai, K.; Hersh, L. B.; MacDonald, P. C. *J. Biol. Chem.* **1991**, *255*, 23041.
16. Oefner, C.; Roques, B. P.; Fournie-Zaluski, M. C.; Dale, G. E. *Acta Crystallogr.* **2004**, *D60*, 392.
17. Berger, J. B. US 4,721,726, 1988.
18. De Lombaert, S.; Erion, M. D.; Tan, J.; Blanchard, L.; El-Chehabi, L.; Ghai, R. D.; Sakane, Y.; Berry, C.; Trapani, A. J. *J. Med. Chem.* **1994**, *37*, 498.
19. Lee, M. R.; Duan, Y.; Kollman, P. A. *Proteins: Struct. Funct. Genet.* **2000**, *39*, 309.
20. Wang, J.; Morin, P.; Wang, W.; Kollman, P. A. *J. Am. Chem. Soc.* **2001**, *123*, 5221.
21. Swanson, J. M. J.; Henchman, R. H.; McCammon, J. A. *Biophys. J.* **2004**, *86*, 67.
22. Case, D. A.; Darden, T. A.; Cheatham, T. E., III; Simmerling, C. L.; Wang, J.; Duke, R. E.; Luo, R.; Merz, K. M., Jr.; Pearlman, D. A.; Crowley, M.; Walker, R. C.; Zhang, W.; Wang, B.; Hayik, S.; Roitberg, A. E.; Seabra, G.; Wong, K. F.; Paesani, F.; Wu, X.; Brozell, S.; Tsui, V.; Gohlke, H.; Yang, L.; Tan, C.; Mongan, J.; Hornak, V.; Cui, G.; Beroza, P.; Mathews, D. H.; Schafmeister, C.; Ross, W. S.; Kollman, P. A. *AMBER 9*; University of California: San Francisco, 2006.
23. Gohlke, H.; Kiel, C.; Case, D. A. *J. Mol. Biol.* **2003**, *330*, 891.
24. Still, W. C.; Tempczyk, A.; Hawley, R. C.; Hendrickson, T. *J. Am. Chem. Soc.* **1990**, *112*, 6127.
25. Ryde, U. *Proteins* **1995**, *21*, 40.